The 2010 IEEE/RSJ International Conference on
Intelligent Robots and Systems
October 18-22, 2010, Taipei, Taiwan

Online Footprint Imitation of a Humanoid Robot by Walking Motion Parameterization

Sung-Kyun Kim, Seokmin Hong, Doik Kim, Yonghwan Oh, Bum-Jae You and Sang-Rok Oh

Abstract— **There are many difficulties in operating a humanoid which has high degree-of-freedom and instability in balancing its body. In addition, due to the shape of a humanoid, it is expected to have motions like a human. In order to overcome its operational difficulties and to provide a human-like motion, a teleoperation with the motion imitation is studied in this paper. Specifically, a framework for online generation of a footprint from a human walking motion is proposed. The human walking motions acquired from a motion capture device are parameterized and normalized to give a human independent foot motion. The normalized parameters are restored by a humanoid considering its hardware limit. The restored footprints generate a walking trajectory of a humanoid, which imitates the human walking motion in terms of the footprint. Experiments are conducted with MAHRU-R, a humanoid robot developed in KIST.**

I. Introduction

In teleoperation of a humanoid, there are two difficult control features compared with other robot systems, i.e. control of high DOF system and self-balancing ability. Since a humanoid usually has more than thirty DOFs and many branches in its body, it is not easy to control every joint or branch simultaneously by buttons, levers or joysticks. Sian *et al.*, used a joystick to map commands to corresponding tasks, but a variety of task mappings and more intuitive interface for the user were expected [1].

For more complicated and various tasks, human motion capture equipments are used as a control input device for the humanoid teleoperation. The inertial measurement units (IMU) are used for NASA Robonaut [2], and the flexible sensor tube (FST) is used for Wakamaru by Mitsubishi [3] for teleoperation of upper body motions. An exoskeleton system is another type of the motion capture equipment, which used in teleoperation of Sarcos [4], [5].

Unlike other input devices such as a joystick, the motion capture equipment can give human-like motion, and thus the motion capture equipment is one of promising motion/command input devices in spite of its weakness in portability and installation.

Locomotion and manipulation are the essential parts in humanoid teleoperation, and are definitely based on self-balancing ability. Due to this balancing problem, it is hard to imitate human walking motion. HRP-2 developed in AIST executed a mobile manipulation task with whole-body balancing, according to the user's command by a joystick [6]. There was another attempt of offline walking motion imitation by remixing human's motion data adequately for a humanoid [7].

Because a human and a humanoid have different kinematic and dynamic characteristics, the humanoid motion may become deviated from the original human walking motion. With this confliction between balance and imitation, online walking imitation is not attempted so far.

This paper is organized as follows: section II briefly explains the full procedure of the walking motion imitation we are studying, and section III explains the footprint imitation scheme of the human walking. Section IV and V describe online walking motion detection scheme and restoration of walking motion for a humanoid, respectively. In section VI, the experimental results are discussed, and section VII concludes this paper.

II. Walking Imatation Procedure

In order to imitate human's walking motion, two major problems occur: 1) a structural gap and 2) a control scheme. Due to the structural gap between a human and a humanoid, walking speed, step size, and so on are quite different from each other, and it is hard to imitate human's walking motion thoroughly. Instead, a humanoid can imitate a relative walking motion of a human within its structural limitation.

In addition to the classical motion imitation problem, a control scheme for guaranteeing the balance needs to be considered, since human and humanoid are contacting the ground with their feet in most cases. A contact situation of a human is very complicated, and the most contact situations, such as walking with high heels, dancing motion, etc., are in partial contact. Even in a normal walking motion, foot uses a partial contact of heel and toe. These contact situations cannot be transferred to a humanoid by the simply mirrored motion only, since the contact is highly dependent on the balance, and in most cases a humanoid cannot guarantee the balanced motion with a partial contact. Moreover, most walking control schemes developed so far do not give walking motion with the knees straightened because of the singularity, except a few humanoids [8]. If the walking motion is imitated with joint angle relations with usual motion imitation methods, the leg shape can imitate a human leg motion well, but the contact situation or balance cannot be guaranteed. With these control problems, it is hard to imitate a walking motion in real time.

Sung-Kyun Kim, Doik Kim, Yonghwan Oh, Bum-Jae You and Sang-Rok Oh are with the Cognitive Robotics Center in Korea Institute of Science and Technology (KIST), Korea {kimsk,doikkim,oyh,ybj,sroh}@kist.re.kr

Seokmin Hong is with Korea University of Science and Technology (UST) and the Cognitive Robotics Center in Korea Institute of Science and Technology (KIST), Korea doberman77@gmail.com

In order to achieve this online walking motion imitation, we are studying it in two ways. One is to imitate footprints.

Footprint imitation:

1) **(imitation)** foot motion detection and restoration in the step wise: The footprints are imitated, and thus a humanoid can follow the human's steps.
2) **(imitation, control)** foot motion detection and restoration by tracking the swinging foot: A swinging foot motion is imitated.
3) **(control)** walking control with a straight knee: A humanoid can walk with a straight knee, and then the footprint imitation can give more natural imitative walking motion.

With this footprint imitation, it is easy to guarantee the balanced motion, but is hard to imitate the leg motion.

The other way is to imitate leg motion with joint relations.

Leg shape imitation:

1) **(imitation, control)** leg shape imitation with joint angles under a predefined contact: A leg shape is fully imitated and the contact situation is limited to the predefined contact situation.
2) **(control)** leg shape imitation with joint angles under a natural contact: A leg shape is fully imitated and the contact situation is not predefined.

With this leg shape imitation, a human leg shape can be imitated well, but it is hard to guarantee the balanced motion of a humanoid. In order to imitate the human walking motion thoroughly, these two approaches are needed to be developed simultaneously, as shown in Fig. 1. Currently, this paper deals with the online footprint imitation, which is the first step of the walking motion imitation.

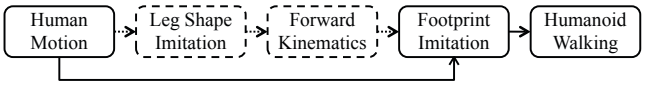

Fig. 1. Overall procedure of the walking motion imitation

III. Footprint Imitation Scheme

Footprint imitation is mainly composed of three processes: walking motion detection from human's motion capture data, walking motion parameterization for step-wise motion, and walking motion resotration in the humanoid to walk, as shown in Fig. 2.

a) Walking motion detection process: Motion capture data of feet poses are investigated first. This process detects supporting/swinging status of each foot, current stance, walking period, swinging foot height. One step is detected after a human finishes his step, and thus time delay of one step at least occurs for humanoid's walking motion.

b) Walking motion parameterization: If the stance is detected to be changed, the walking motion parameterization process is conducted. Normalized Walking Motion Parameters (NWMP) are defined as follows:

$$\text{NWMP} = (\eta_{SSL}, \eta_{FSL}, \theta, \eta_{FH}, STN, T_{period}) \qquad (1)$$

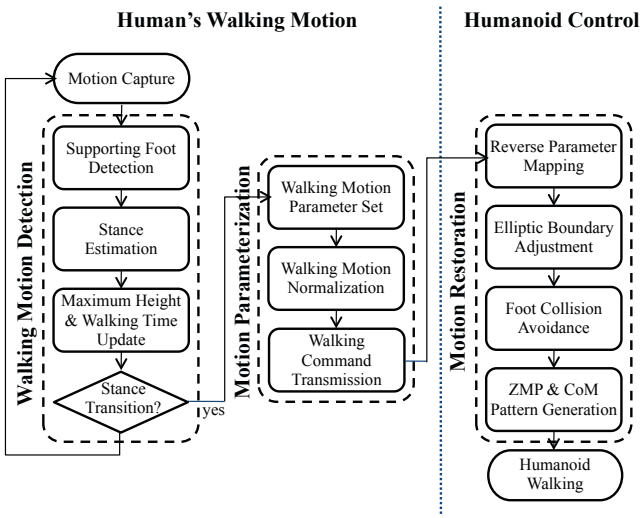

Fig. 2. Procedure of the footprint imitation

where η_{SSL} and η_{FSL} are normalized sagittal and frontal step length, θ is foot angle of swing foot, η_{FH} is normalized height of swing foot, STN is stance and T_{period} is current step period, respectively. With this normalized parameters, the foot motion can be restored within the limit of a target humanoid hardware. In order to represent a walking motion with these six parameters, it is assumed that the swing foot has a sinusoidal motion, not an arbitrary motion in the air.

c) Walking Motion Restoration: In the humanoid, by reverse mapping of the NWMP according to the humanoid's ability, the footprint is restored. However, this footprint may not be adequate for the robot due to the discrepancy between the human and the robot. Thus, the restored footprint is modified to guarantee the balance of a robot.

IV. Human Walking Detection

A. Supporting Foot Detection

Supporting Foot Detection (SFD) is in charge of checking supporting/swinging state of each foot for every motion capture data. The result of SFD is used in Stance Estimation (SE) to decide the current stance is left-support, right-support or double-support [9].

There would be an argue about what feature of data is the most suitable. Since IMU sensor has accumulative drift error, foot position and orientation themselves are not quite reliable. Thus, it is better to use relative than to use absolute values. In SFD, the norm of linear foot velocity, i.e. foot speed, is used as a feature.

The essence algorithm of SFD is described in Algorithm 1, which is already introduced in [9]. x_i denotes 3D foot position vector at time i, Δt is sampling period, s_{spp} is *maximum supporting foot speed*, t_{spp} is *minimum supporting time*, and n is supporting time counter.

Let $X(i) = \{x_{i-n_{thr}}, \cdots, x_i\}$ be a sequence of foot position, and $V(i) = \{s_{i+1-n_{thr}}, \cdots, s_i\}$ be a sequence of foot speed.

Algorithm 1 Supporting foot detection

if $\frac{\|x_i - x_{i-1}\|}{\Delta t} \leq s_{spp}$ **then**
  n $\leftarrow$ n+1
else
  n $\leftarrow$ 0
end if
if $n \geq n_{thr} = \left[\frac{t_{spp}}{\Delta t}\right]$ **then**
  Foot State $\leftarrow$ *Supporting*
else
  Foot State $\leftarrow$ *Swinging*
end if

Note that Δt is a constant value, which is 10 ms in implementation, and foot speed, s_i, is the mean speed for interval Δt. Provided that *Foot State* is *Supporting* at time i, (2) is satisfied.

$$s_k \leq s_{spp} \ for \ ^{\forall}s_k \in V(i), \ k = i+1-n_{thr}, \cdots, i \qquad (2)$$

Then, interval mean speed, $\bar{s}_i$, for interval t_{spp} satisfies (3).

$$\bar{s}_i = \frac{s_{i+1-n_{thr}} + \cdots + s_i}{[t_{spp}/\Delta t]} \leq s_{spp} \qquad (3)$$

In the aspect of analysis process, $\bar{s}_i$ in (3) is more tractable than s_k in $V(i)$ in (2). Since (3) is a necessity condition of (2), the design of SFD using (3) would give more conservative classification rule for (2). Thus, analysis hereafter regards only $\bar{s}$, not s_k in $V(i)$.

As shown in (3), there are two design parameters in the algorithm, i.e. s_{spp} and t_{spp}. In order to determine these values, statistical analysis using practical data is prerequisite, since IMU sensor data are sensitive to experimental environment such as magnetic field disturbances and sensor mount condition.

B. Statistical Design of Supporting Foot Detection

Statistical characteristics of human's walking motion are investigated with motion capture data. Elementary walking motions in sagittal and frontal directions are used for analysis. Each motion is composed of ten steps, and the walking speed is about 0.5 m/s. In order to obtain statistical characteristics of supporting state and swinging state, respectively, foot states of all sampling data are classified manually. Supporting state class and swinging state class are denoted by S_{spp} and S_{swg}, respectively.

With an assumption that $\bar{s}$ is a random variable of Gaussian distribution, two-class statistical decision making method is applied to determine the design parameters[10].

The analysis process is as follows:

1) compute $\bar{s}$ for different interval length, i.e. t_{spp}
2) obtain probability density function (PDF) of $\bar{s}$
3) compare PDFs of S_{spp} and S_{swg}
4) find the intersection point, $\bar{s}_d$, i.e. s_{spp}

PDFs of S_{spp} and S_{swg} have the same probability at $\bar{s}_d$, which is called discriminant value. This means that $\bar{s}$ less than $\bar{s}_d$ is probably in different state class with $\bar{s}$ larger than $\bar{s}_d$. Thus, $\bar{s}_d$ can be used as classification threshold, i.e. s_{spp}, and of course, the corresponding interval is t_{spp}.

$\bar{s}_d$ can be obtained from (4), where μ and σ stand for the mean and the standard deviation, and $(\cdot)_{spp}$ and $(\cdot)_{swg}$ imply supporting state and swinging state.

$$P(S_{spp})\frac{1}{\sigma_{spp}\sqrt{2\pi}}e^{-\frac{1}{2}\left(\frac{\bar{s}_d-\mu_{spp}}{\sigma_A}\right)^2} = P(S_{swg})\frac{1}{\sigma_{swg}\sqrt{2\pi}}e^{-\frac{1}{2}\left(\frac{\bar{s}_d-\mu_{swg}}{\sigma_B}\right)^2} \qquad (4)$$

The analysis for four different t_{spp} is conducted and presented in the followings. In Fig. 3, PDFs of $\bar{s}$ are depicted. $\bar{s}$ of S_{spp} has high probability at zero, while that of S_{swg} has almost even probability in wide interval speed region.

In Table I, μ and σ for each t_{spp} have been computed. It is found that σ_{spp} is getting smaller as t_{spp} increases up to 100 ms, because the sensor noise is filtered off by longer interval length. However, for 200 ms interval window, there would be overlapped region with supporting and swinging foot, so that σ_{spp} has rather larger value.

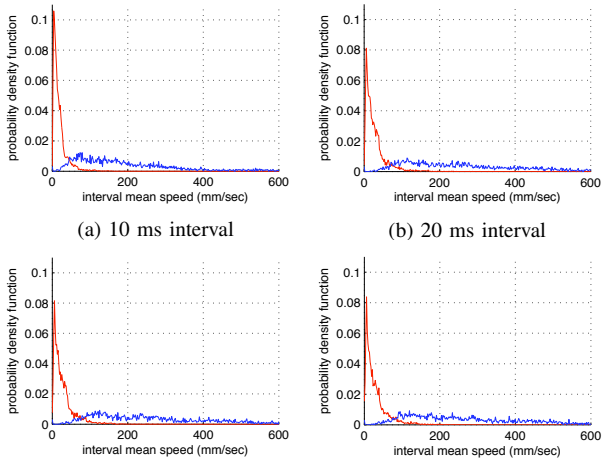

(a) 10 ms interval (b) 20 ms interval

(c) 100 ms interval (d) 200 ms interval

Fig. 3. Velocity of supporting foot (red) and swinging foot (blue)

TABLE I
MEAN AND STANDARD DEVIATION

Interval Length (t_{spp}) [ms]		10	50	100	200
Supporting State	Mean (μ_{spp}) [mm/s]	31.0	30.1	29.8	30.3
	Std.dev. (σ_{spp}) [mm/s]	1.2	1.1	1.0	1.2
Swinging State	Mean (μ_{swg}) [mm/s]	315.6	310.4	303.2	286.3
	Std.dev. (σ_{swg}) [mm/s]	47.5	44.7	42.3	36.5

According to the analysis results, the design parameters of SFD are determined. In order to find the most suitable parameter values, detection accuracy is measured for each interval length as depicted in Table II. The detection accuracy test shows that 36.7 mm/s of s_{spp} with 100 ms of t_{spp} are the most suitable design parameters.

TABLE II
DETECTION ACCURACY

Min. spp. time (t_{spp}) [ms]	10	50	100	200
Min. spp. time count (n_{thr})	1	5	10	20
Max. spp. ft. speed (s_{spp}) [mm/s]	38.7	37.5	36.7	39.0
Supporting State [%]	74.2	74.4	75.5	74.7
Swinging State [%]	99.2	99.3	99.3	98.8

C. Walking Motion Parameter Normalization

The detected walking motion is not adequate for a humanoid to walk, since human individuals have various patterns of walking, and the robot has its own walking capability which is much inferior to those of humans. Thus, walking motion parameters are normalized with respect to the human's walking pattern, and restored in the humanoid according to its own specifications.

The parameters concerned in the normalization process are sagittal step length (L_{SSL}), frontal step length (L_{FSL}), and height of swinging foot (L_{FH}). Statistical data of normal step length (L_{NSL}) and normal swinging foot height (L_{NFH}) are found in [10], [11].

L_{NSL} has a correlation with ages and heights, respectively. In order to estimate L_{NSL} for a human, mapping function from age and height to L_{NSL} is built as in Fig. 4. Since the data set is quite limited, spline interpolation is used to build this mapping function.

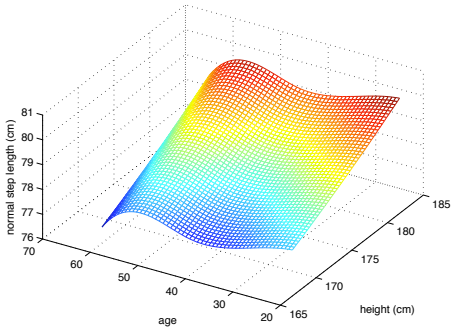

Fig. 4. Mapping of normal step length with respect to age and height

L_{NFH} varies in wide region according to walking situations such as obstacles. In the normalization process, L_{NFH} is set as 31.1 mm, which is obtained from young adults of middle heights.

If preliminary information about the human is provided, L_{NSL} and L_{NFH} are estimated, and the normalized walking parameters (η) are obtained as follows.

$$\eta_{SSL} = L_{SSL}/L_{NSL} \quad (5)$$

$$\eta_{FSL} = L_{FSL}/L_{NSL} \quad (6)$$

$$\eta_{FH} = L_{FH}/L_{NFH} \quad (7)$$

V. RESTORATION OF IMITATED FOOT PRINT

In this section, we explain the method used for restoring walking motion from NWMP. The restored footprints are not implemented directly by the robot, but by considering their geometrical difference between human and robot. A proper swinging foot position will be decided through the elliptic adjustment and collision detection procedure. Fig. 5 shows the overall block diagram for walking motion restoration.

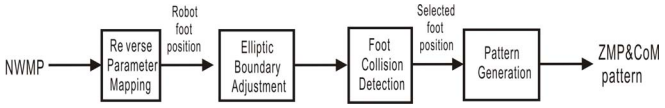

Fig. 5. Overall block diagram for restoring walking motion from NWMP

A. Reverse Parameter Mapping

As mention above, NWPM is normalized data from human walking. A data is restored by considering robot's mechanical constraints, because every humanoid has a different mechanical specification. The regeneration can represented as following:

$$l_{SSL} = \eta_{SSL} \cdot l_{SSLmax} \quad (8)$$

$$l_{FSL} = \eta_{FSL} \cdot l_{FSLmax} \quad (9)$$

$$l_{FH} = \eta_{FH} \cdot l_{FHmax} \quad (10)$$

where the terms on the left side mean walking parameters used for a humanoid. The first terms on the right side mean the normalized walking parameter from NWPM. And the second terms on the right side of equations are obtained by the robot mechanical limit.

B. Elliptic Boundary Adjustment

The restored parameters l_{SSL}, l_{FSL} in (8), (9) consist of the position of swinging foot. But the position should be checked from the workspace's point of view. If two positions are combined, the foot position can be outside the workspace. To overcome this problem, the swinging foot positions are constrained inside a specific area, for example, an ellipse. The elliptic area in Fig. 6 is constituted with maximum SSL and maximum FSL. In Fig. 6, superscript 'ori' describes the original foot position and superscript 'mod' represents the modified foot position by the elliptic area.

The center of ellipse is the swinging foot position if it is standstill as the first initial position. The ellipse is represented by

$$\frac{x^2}{{l_{SSLmax}}^2} + \frac{y^2}{{l_{FSLmax}}^2} = 1 \quad (11)$$

where x and y describe position values about swinging foot with respect to the center of the ellipse.

If the foot position is inside the ellipse, the foot position can be implementable for walking pattern. If the foot position is outside the ellipse, however, the foot position must be modified inside the ellipse, because this elliptic area represents the reaching area by swinging foot including the

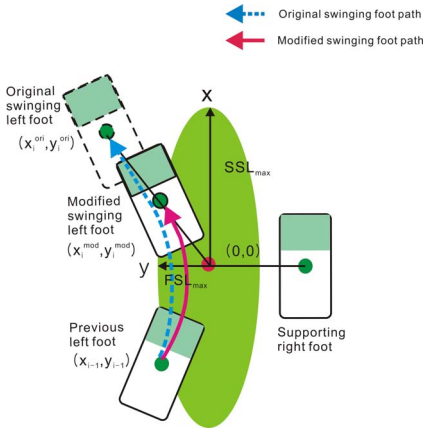

Fig. 6. Selecting foot position applied to elliptic area

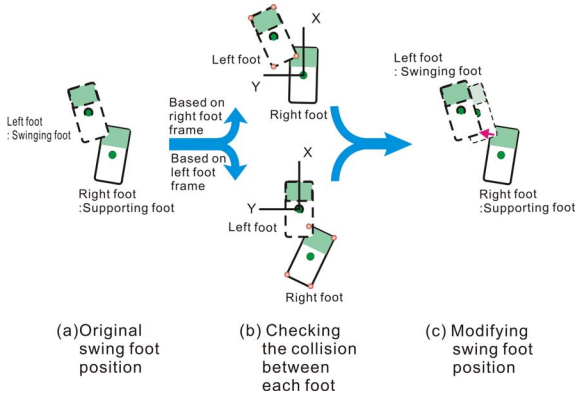

Fig. 8. Checking the collision and modifying swing foot position (in the case of left foot swinging)

robot kinematical constraints. The modified position can be obtained by the intersection point between the ellipse and the line which passes from center to the the ellipse.

The modified position of swinging foot is represented like

$$x_i^{mod} = \frac{l_{SSLmax} \cdot l_{FSLmax} \cdot x_i^{ori}}{\sqrt{(l_{FSLmax} \cdot x_i^{ori})^2 + (l_{SSLmax} \cdot y_i^{ori})^2}} \quad (12)$$

$$y_i^{mod} = \frac{l_{SSLmax} \cdot l_{FSLmax} \cdot y_i^{ori}}{\sqrt{(l_{FSLmax} \cdot x_i^{ori})^2 + (l_{SSLmax} \cdot y_i^{ori})^2}} \quad (13)$$

This modified foot positions satisfy the robot's kinematic limit and human walking intent properly.

C. Foot Collision Detection

Unlike human's walking motion, a robot should not collide inside its body. In our case, the foot collision needs to be avoided. Fig. 7 shows the collision examples inside each foot. We assume each foot of the robot is regarded as a rectangle for simplification. To detect the collision of feet simply and quickly, four corners of each foot are inspected whether any corner of one foot is inside the other foot area and vice versa, as shown in Fig. 8 (b). In the case that the collision is detected, the swinging foot is shifted by the predefined distance from the supporting foot as shown in Fig. 8 (c).

In the case that the collision is detected, the swinging foot is shifted to some distance from the supporting foot as shown in Fig. 8 (c) to avoid the collision.

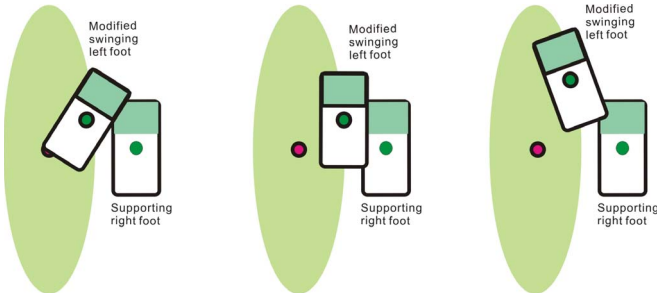

Fig. 7. Collision examples between swinging foot and supporting foot

D. Generating the Walking Pattern

In order to generate a walking pattern from the restored foot position, a feedforward and a feedback controller for a humanoid walking are utilized as shown in Fig. 9 [12]. Firstly, the feedback controller stabilizes the linear inverted pendulum model more. For this purpose, the pole placement method is used as feedback controller. Secondly, the feedforward controller improves the tracking performance. Especially this feedforward controller reduces the effect of the the unstable zero which is located out of unit circle in Z domain. We utilize the advanced pole-zero cancelation by series approximation(APZCSA) controller. This controller can approximate the inverse of a unstable zero by using the series approximation. The steady state error can be reduced by adding to $1/(z_u^{Norder} - 1)$ as shown in Fig. 9. The stable patterns of the ZMP and the CoM are generated by these two controllers.

The obtained pattern the ZMP and the CoM are transmitted to a humanoid robot.

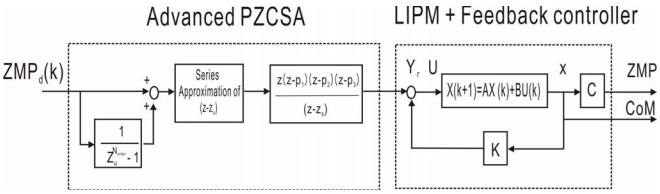

Fig. 9. Block diagram for generating walking pattern with APZCSA

VI. Experimental Result

To validate the proposed online footprint imitation method, experiments are conducted with MAHRU-R, a humanoid of KIST. MVN System of Xsens Technologies B.V., is used for the IMU motion capture system [13]. It has 16 IMU sensors on the sensor suit, and offers human's full-body motion data which are anatomically reconstructed based on raw data from the IMU sensors. The resolutions of IMU are 0.05 deg. in 3D orientation, 2 mg in acceleration, 0.6 deg/sec in gyroscope. The maximum streaming rate is 120 Hz.

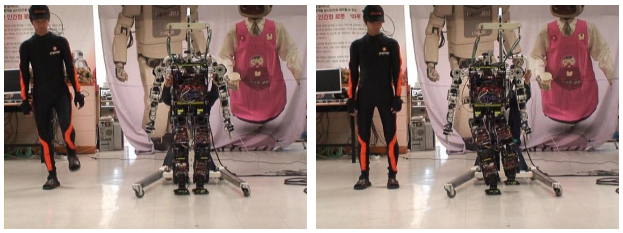

Fig. 10. Online footprint imitation experiment

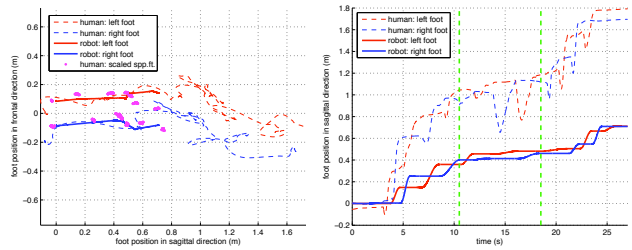

(a) position in transversal plane (b) position in sagittal direction

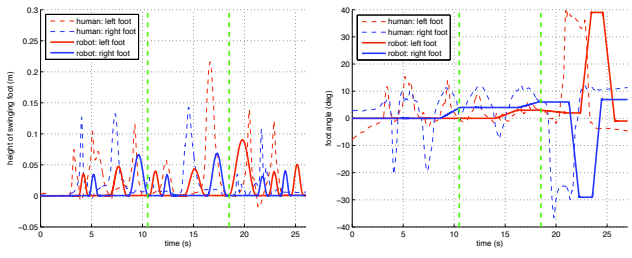

(c) height of swinging foot (d) foot angle

Fig. 11. Experiment of footprint imitation for forward walking

Fig. 10 shows the practical experiment for the footprint imitation. In the experiment, the human subject is asked to walk in three sequential motions: forward walking with short and long periods, marking time with low and high swinging heights, and forward walking with wide and narrow foot angles.

Fig. 11 shows the experimental results of footprint imitation. In Fig. 11(a), locomotion of the human and the robot is depicted. Due to the difference of walking capabilities, the walking paths do no match. In order to compare the shape of walking paths, human's footprints are scaled down. The scaled path is similar to the robot's path, except the end of paths near (0.6 m, 0.1 m) in the figure. The reason is that the robot's footprint is modified to avoid foot collision, because the human's footprints are too close. Note that the robot's motions are delayed about one step, because of the foot step detection.

In Fig. 11(b), (c), and (d), foot position in the sagittal direction, height of swinging foot and foot angle are shown with respect to time. All variations in the walking motion are well reflected to the robot's walking motion.

In the aspect of stability, the result is more admirable. As shown in Fig. 11(b), there is backswing in the human's walking data. This is because the the IMU motion capture device are influenced by magnetic field disturbance and drift error. However, footprint detection is quite robust despite the data distortion, and the resultant robot's walking imitation does not cause any stability problems.

VII. Conclusion

Online footprint imitation with walking motion parameterization is proposed as the first step of walking motion imitation. The footprint imitation, composed of walking motion detection, parameterization and restoration, is explained focusing on several essential processes. Experiment validated the proposed method that human foot motion in step length, foot angle, swinging foot height and walking period.

As further works, swinging foot trajectory, which is assumed to be sinusoidal in this paper, should be imitated online. The issue on swinging foot trajectory is how to remove sensor disturbance and extract stable trajectory motion. Leg motion imitation control with a straight knee would be the final goal. It requires a humanoid to walk with its knee straightened and to maintain balance while fully imitating a human's leg motion. In the near future, we would improve our method with stability as well as joint imitation, and finally develop online leg shape imitation.

References

[1] N.E. Sian, K. Yokoi, S. Kajita, F. Kanehiro, and K. Tanie, "Whole body teleoperation of a humanoid robot development of a simple master device using joysticks", *JOURNAL-ROBOTICS SOCIETY OF JAPAN.*, vol. 22, no. 4, pp. 97–105, 2004.

[2] N. Miller, O.C. Jenkins, M. Kallmann, and M.J. Mataric, "Motion capture from inertial sensing for untethered humanoid teleoperation", in *Proc. 4th IEEE/RAS International Conference on Humanoid Robots (Humanoids 2004)*. Citeseer, 2004, vol. 2, pp. 547–565.

[3] http://www.mhi.co.jp/kobe/wakamaru/english/, ".

[4] S. Tachi, "Real-time remote robotics—Toward networked telexistence", *IEEE Computer Graphics and Applications*, pp. 6–9, 1998.

[5] N.S. Pollard, J.K. Hodgins, M.J. Riley, and C.G. Atkeson, "Adapting human motion for the control of a humanoid robot", in *Proceedings-IEEE International Conference on Robotics and Automation*. Citeseer, 2002, vol. 2, pp. 1390–1397.

[6] Mike Stilman, Koichi Nishiwaki, and Satoshi Kagami, "Humanoid Teleoperation for Whole Body Manipulation", in *Proceedings of the IEEE Int. Conf. on Robotics and Automation*, 2008.

[7] Kanako Miura, Mitsuhara Morisawa, Shin'ichiro Nakaoka, Fumio Kanehiro, Kensuke Harada, Kenji Kaneko, and Shuuji Kajita, "Robot motion remix based on motion capture data - towards human-like locomotion of humanoid robots -", in *Humanoid Robots, 2009. Humanoids 2009. 9th IEEE-RAS International Conference on*, 2009, pp. 596 – 603.

[8] Yu Ogura, Kazushi Shimomura, Hideki Kondo, Akitoshi Morishima, Tatsu Okubo, Shimpei Momoki, Hun ok Lim, and Atsuo Takanishi, "Human-like walking with knee stretched, heel-contact and toe-off motion by a humanoid robot", in *IROS*, 2006, pp. 3976 – 3981.

[9] Sung-Kyun Kim, Seokmin Hong, and Doik Kim, "A walking motion imitation framework of a humanoid robot by human walking recognition from imu motion data", in *Humanoid Robots, 2009. Humanoids 2009. 9th IEEE-RAS International Conference on*, 2009, pp. 343 –348.

[10] E. Gose, R. Johnsonbaugh, and S. Jost, *Pattern recognition and image analysis*, Prentice Hall, 1996.

[11] L.S. Chou and L.F. Draganich, "Stepping over an obstacle increases the motions and moments of the joints of the trailing limb in young adults", *Journal of biomechanics*, vol. 30, no. 4, pp. 331–337, 1997.

[12] Seokmin Hong, Yonghwan Oh, Doik Kim, and Bum-Jae You, "A walking pattern generation method with feedback and feedforward control for humanoid robots", in *IROS*, 2009, pp. 1078 – 1083.

[13] D. Roetenberg, H. Luinge, and P. Slycke, "Moven: Full 6DOF Human Motion Tracking Using Miniature Inertial Sensors", *Xsen Technologies, December*, 2007.